Chapter 3

Experimental Methods

3.1 Gas Adsorption Measurements

3.1.1 Introduction

To characterize a potential hydrogen storage material, we must measure the amount of hydrogen it adsorbs at various temperatures and pressures. The adsorption amount is typically measured as a function of pressure while the temperature is held constant. These isothermal pressure-composition curves are called "isotherms". Two important quantities can be derived from the isotherm: (a) the maximum adsorption capacity, and (b) the isosteric heat of adsorption. The heat of adsorption is particularly significant as an indicator of the interaction strength between the hydrogen molecules and the adsorbent host.

3.1.2 Theoretical framework

3.1.2.1 Surface excess adsorption

Quantifying the amount of an adsorbed gas is a deceptively subtle task. The important quantities pertaining to a solid/gas interface are illustrated in Fig. 3.1. Near the adsorbent surface, in the region labeled "adsorbed layer", the local adsorptive density is considerably

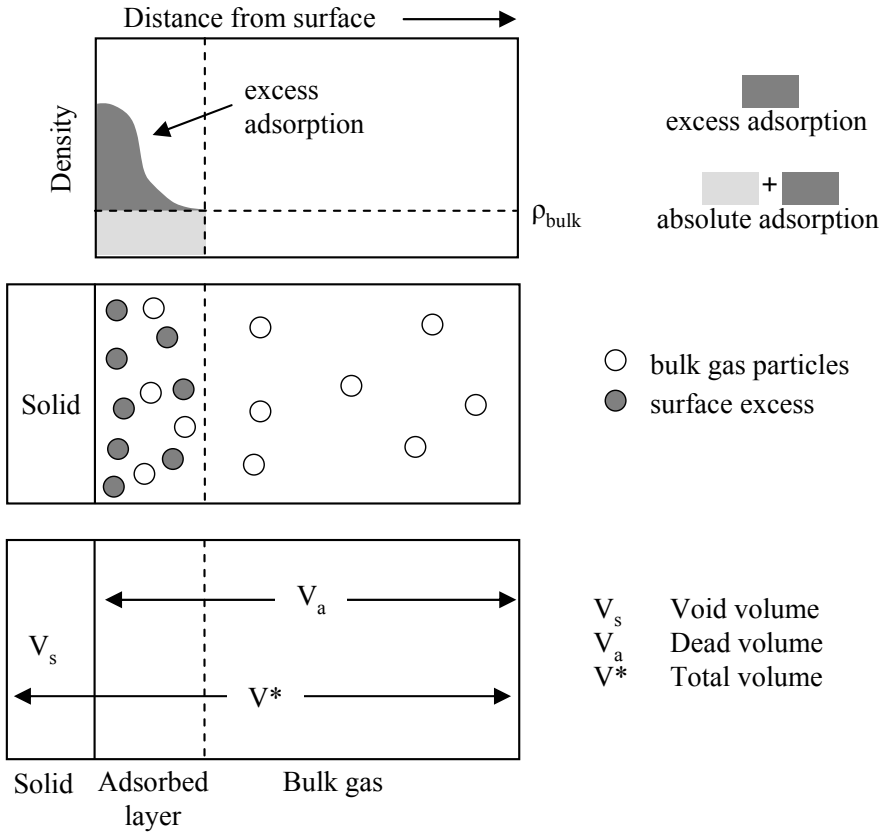

Figure 3.1: Illustration of surface excess adsorption and absolute adsorption. (Top) Density profile of the adsorptive gas as a function of distance from the adsorbent surface. Dark gray areas denote the adsorbed molecules, whereas light gray areas represent bulk gas amounts which are not counted towards adsorption in the surface excess scheme. (Middle) Illustration of the concept of bulk and adsorbed molecules. (Bottom) Important volumes of the adsorption system.

Table 3.1: Important definitions for adsorption

Symbol	Description
n^*	The total amount of adsorptive in the system (both adsorbed and bulk)
V^*	The total volume of the system (including the volume occupied by the adsorbent). It is known by calibrating the instrument.
V_s	The "void volume." This is the volume of the solid which is impenetrable for the adsorptive gas. It is typically measured by helium pycnometry.
m_s	Mass of the adsorbent.
V_a	The "dead volume." It is the difference between the total system volume and the void volume, $V_\mathrm{a} = V^* - V_\mathrm{s}$.

[a] *Adsorptive* refers to the chemical identity of the adsorbed and bulk molecules interacting with the adsorbent surface. *Adsorbate* refers specifically to the adsorbed molecules. Only a single-component adsorptive is considered here.

higher than in the bulk gas phase.[1] It is assumed that at a suitably large distance from the adsorbent surface, the adsorptive density decays back to a constant bulk density (ρ_{bulk}). This region is labeled as the "bulk gas." Important quantities for the adsorption model are defined in Table 3.1.

The standard practice is to express adsorption as a Gibbs *surface excess* quantity. This is the amount of adsorptive which is present in the adsorbed layer in excess of the bulk gas density, indicated in Fig. 3.1 by the dark gray region. Conveniently, the surface excess amount is the quantity which is measured in a standard volumetric measurement. The expression for the Gibbs surface excess amount is therefore

$$n^{\sigma} = n^{*} - \rho_{\text{bulk}} V_{\text{a}}. \tag{3.1}$$

The surface excess amount n^{σ} is an extensive quantity. Typically, however, data are presented as a specific surface excess amount

$$n = n^{\sigma}/m_s, \tag{3.2}$$

where m_s is the sorbent mass. It is also common to present the excess adsorption as a weight percent,

$$n(\text{wt}\%) = \left(\frac{m^{\sigma}}{m_s}\right) \times 100, \tag{3.3}$$

where m^{σ} is the surface excess mass. Both formats are used interchangeably in this thesis depending on the context.[2]

[1] This density profile is not known experimentally.

[2] It may seem attractive to consider the *absolute adsorption* amount, which is the total number of adsorptive molecules that are located within the adsorbate volume V_{ad}. However, V_{ad} cannot be measured directly since the density profile is not experimentally known. From an engineering viewpoint, therefore, the absolute adsorption amount is not particularly useful. It can be approximated as $n^{\text{a}} = n^{\sigma} + \rho_{\text{bulk}} V_{\text{ad}}$,

Most hydrogen adsorption measurements are performed well above the critical temperature of hydrogen (33 K). Supercritical H_2 cannot be liquefied by increasing the pressure, and therefore there is no saturation pressure. Consequently, hydrogen adsorption isotherms can extend up to high pressures and are often denoted "high-pressure isotherms." Supercritical isotherms often exhibit a local maximum when plotted versus pressure [73]. Above a certain pressure the bulk density begins to increase faster than the adsorbate density, and the excess adsorption actually decreases. Supercritical isotherms are characterized by monolayer adsorption and by a general decrease of the maximum adsorption amount with temperature [73].

3.1.2.2 Thermodynamics

A complete thermodynamic theory can be developed for a surface excess phase in equilibrium with a bulk gas phase, and a brief summary is provided here. The equations, notation, and terminology used in this section are taken directly from Ref. [6]. The surface excess layer can be considered as a distinct phase, with a thermodynamic state that is completely characterized by an area A, a spreading pressure Π, and a surface excess concentration $\Gamma = n^\sigma/A$. The differential energy of adsorption is the change in internal energy of the entire adsorption system upon the addition of an infinitesimal surface excess amount $\mathrm{d}n^\sigma$. In principle this can be measured directly by calorimetry. A more useful quantity is the differential enthalpy of adsorption ($\Delta\dot{h}_{T,\Gamma}$), which can be measured indirectly by the isosteric method. From the equilibrium condition between the surface excess phase and the bulk gas

where V_{ad} is approximated as the specific pore volume determined from surface texture analysis. Adsorption amount can also be reported as the total amount of hydrogen contained in the sample vessel [72]. This amount includes both the hydrogen that fills the dead volume of the vessel and the hydrogen that is bound on the adsorbent. Since this number is influenced by both the system volume and the adsorbent packing, it is not useful in describing intrinsic material properties. It may have some use in characterizing system volumetric densities in engineered storage systems, for example.

phase (i.e., $\mu^\sigma = \mu^\mathrm{g}$), the following expression can be derived,

$$\begin{aligned} \ln\left(\frac{p}{p^\circ}\right) &= \frac{\dot{u}^\sigma_{T,\Gamma} - u^\mathrm{g}_T - RT}{RT} - \frac{\dot{s}^\sigma_{T,\Gamma} - s^{\mathrm{g},\circ}_T}{R} \\ &= \frac{\Delta\dot{h}_{T,\Gamma}}{RT} - \frac{\Delta\dot{s}_{T,\Gamma}}{R}, \end{aligned} \tag{3.4}$$

where the differential enthalpy and entropy of adsorption are implicitly defined. The term $s^{\mathrm{g},\circ}_T$ is the standard molar entropy of the ideal gas at the standard pressure $p^\circ = 1$ bar. The quantity u^g_T is the internal energy of an ideal gas particle, and $\dot{u}^\sigma_{T,\Gamma}$ is the differential surface excess internal energy (i.e., the derivative of the total surface excess internal energy with respect to n^σ).

3.1.2.3 Isosteric heat of adsorption

We would like to calculate the differential enthalpy of adsorption from the experimentally measured quantities n^σ, p, and T. This is done using the *isosteric method* where a series of isotherms are measured at different temperatures. Equation 3.4 is differentiated with respect to temperature while holding Γ constant. If we assume that $\Delta\dot{h}_{T,\Gamma}$ and $\Delta\dot{s}_{T,\Gamma}$ are not dependent on temperature, then

$$\left(\frac{\partial}{\partial T}\ln[p]\right)_\Gamma = -\frac{\Delta\dot{h}_{T,\Gamma}}{RT^2}, \tag{3.5}$$

and we obtain,

$$\Delta\dot{h}_{T,\Gamma} = R\left(\frac{\partial \ln[p]}{\partial\,(1/T)}\right)_\Gamma, \tag{3.6}$$

where p is the pressure corresponding to the surface excess concentration Γ. When Eq. 3.6 is used to determine the differential enthalpy, at least two isotherms need to be measured

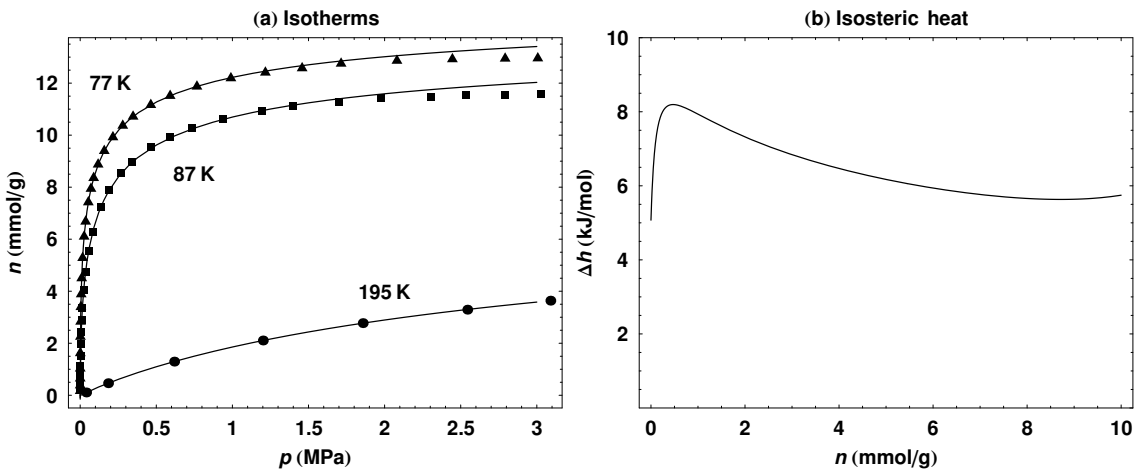

Figure 3.2: Isosteric heat derived from empirical functions fitted independently to each isotherm. (Left) Hydrogen adsorption isotherms of activated carbon CNS-201, each fitted to a Hill equation. (Right) Isosteric heat calculated from the fits (using Eq. 3.7).

at different temperatures which are not too far apart (a separation of 10 K is good).[3] The quantity obtained by this method is sometimes called the *isosteric heat*, to indicate that it has been determined by the isosteric method.

Experimental isotherms are not measured at perfectly spaced n intervals. Therefore it is necessary to either fit the isotherm to some function, or to interpolate the appropriate n from the isotherm data points. Because the isosteric method is very sensitive to errors in the equilibrium pressure, interpolation can sometimes introduce significant artifacts into the calculated isosteric heat. Our standard approach is to fit the 77 K and 87 K isotherms individually to an empirical function, $n = f(p)$. The isosteric heat can now be estimated

[3] It is better to measure more than two isotherms and then plot the isosteres ($\ln p$ versus $1/T$ for a constant value of n) to check for linearity.

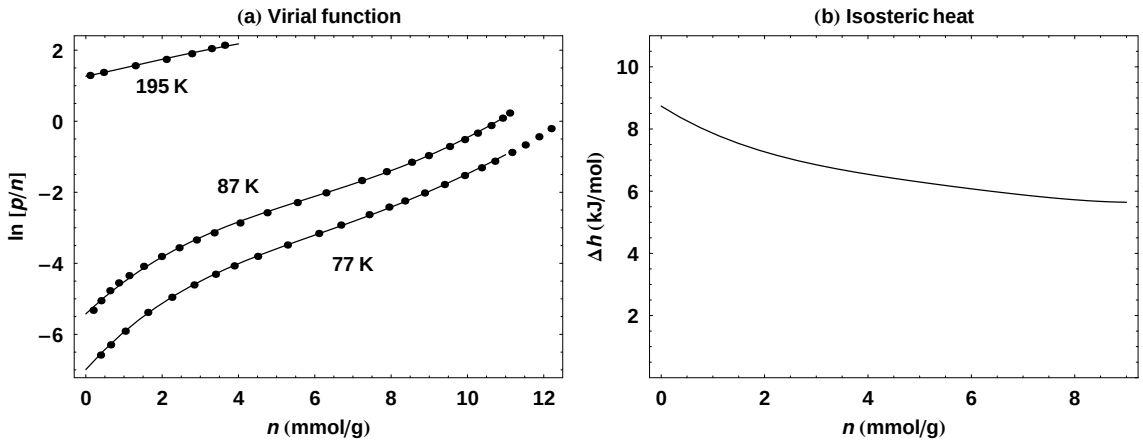

Figure 3.3: (a) Hydrogen adsorption isotherms of CNS-201 fitted to a single model-independent virial equation given by Eq. 3.8. The data is plotted as $\ln[p/n]$ versus n. (b) Isosteric heat calculated from Eq. 3.9.

from the inverse of the fitting functions,

$$\begin{aligned}\Delta\dot{h}_{T,\Gamma} &= R\left(\frac{\partial \ln[p]}{\partial\,(1/T)}\right)_{\Gamma} \\ &\approx \left(\frac{\ln\left[f_{77}^{-1}(n)\right] - \ln\left[f_{87}^{-1}(n)\right]}{(77\,\mathrm{K})^{-1} - (87\,\mathrm{K})^{-1}}\right) \times \left(8.314\,\mathrm{J\,mol^{-1}\,K^{-1}}\right) \\ &= \left(\ln\left[\frac{f_{77}^{-1}(n)}{f_{87}^{-1}(n)}\right]\right) \times \left(5.57\,\mathrm{kJ\,mol^{-1}}\right).\end{aligned} \tag{3.7}$$

The units of the fitting function cancel out in the last expression as long as they are used consistently. One problem with this method is that it is often difficult to fit the experimental isotherms in the low pressure region. This is especially true for the steep isotherms which are typical of microporous adsorbents. An example of the problems with fits to empirical equations at low pressures is illustrated in Fig. 3.2. The 77 K and 87 K hydrogen adsorption isotherms collected on an activated carbon (CNS-201) were individually fitted to the Hill equation.[4] The isosteric heat was calculated from the fits (using Eq 3.7). It is clear that there is an artificial drop in the isosteric heat as n approaches zero.

[4]The Hill equation utilized here is actually equivalent to the Langmuir equation. It is given by $f(p) = n_{\max}/\left[1 + (a/p)^r\right]$, where r sets rate at which the function grows, and a sets the p-value at which the function is at half-maximum.

I found that a better method for calculating isosteric heats is to fit all the hydrogen adsorption isotherms to a single model-independent virial-type thermal equation [74]. This equation is given by

$$\ln p = \frac{1}{T}\sum_{i=0}^{l} a_i n^i + \sum_{i=0}^{m} b_i n^i + \ln n. \tag{3.8}$$

Equation 3.8 is fit simultaneously to the 77 K, 87 K, and 195 K data. Fitting parameters $\{a_i,b_i\}$ are temperature independent, and the sum limits l and m are increased until a sufficient goodness-of-fit is reached. The isosteric heat can be easily calculated from Eq. 3.8 by taking the derivative with respect to T,

$$\Delta\dot{h}_{T,\Gamma} = R\left(\frac{\partial \ln[p]}{\partial\,(1/T)}\right)_{\Gamma} = -R\sum_{i=0}^{l} a_i n^i. \tag{3.9}$$

In the zero-coverage limit the enthalpy equals $\Delta\dot{h}_{T,\Gamma} = -R\,(a_0)$. An example of the model-independent virial equation for the same CNS-201 sample is displayed in Fig. 3.3. The adsorption data is presented in terms of $\ln(p/n)$ versus n and is fit simultaneously to the virial-type thermal equation. Values of $l = m = 5$ were sufficient for the fit. The isosteric heat now has the correct shape in the low pressure region, without the artificial drop obtained from the individual fits to the empirical equation (Eq. 3.7). All of the isosteric heats presented in this thesis were calculated using the model-independent virial equation method, unless otherwise specified.

3.1.2.4 Henry's law

In the low pressure region, surface excess adsorption is proportional to the equilibrium pressure (Henry's law). This is basically a consequence of the dilute adsorbed phase behaving

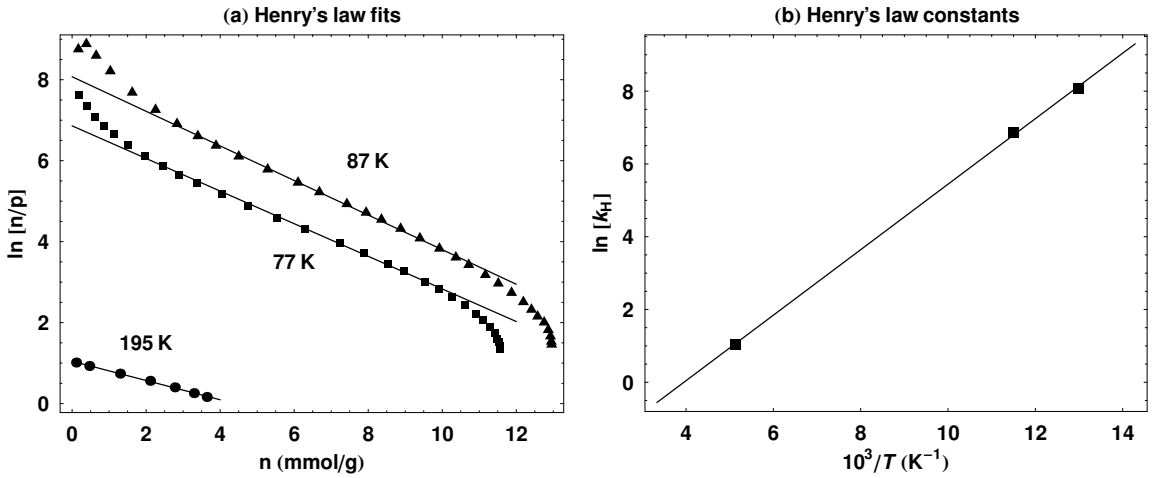

Figure 3.4: Differential enthalpy of adsorption in the zero-coverage limit calculated from Henry's law. (a) Adsorption isotherm points from CNS-201 presented in the $\ln[n/p]$ versus n format. The Henry's law constant for each temperature is equal to the y-intercept of the fitted line. (b) Henry's law constants at 77 K, 87 K and 195 K are plotted against $1/T$.

like a two dimensional ideal gas. The relation is given by

$$n = k_{\mathrm{H}} p, \tag{3.10}$$

where k_{H} is known as the Henry's law constant. To calculate Henry's law constants, adsorption in the low-pressure region can be accurately modeled by a virial-type equation to take into account small deviations from linearity

$$\ln(n/p) = K_0 + K_1 n + K_2 n^2 + \cdots . \tag{3.11}$$

Since $k_{\mathrm{H}} = \lim_{n \to 0} (n/p)$, the Henry's law constant can be obtained from the zero-order virial coefficient $K_0 = \ln(k_{\mathrm{H}})$. By carefully measuring adsorption amounts in the low-pressure region using a high resolution gauge, we can therefore obtain accurate Henry's law constants at 77 K, 87 K, 195 K, and 298 K. An example for the CNS-201 sample is provided in Fig. 3.4. The y-intercepts of the fitted lines are used to calculate the Henry's law constant at each

temperature.[5] The differential enthalpy of adsorption in the limit of zero coverage ($\Delta\dot{h}_0$) can be calculated from the van't Hoff equation

$$\Delta\dot{h}_0 = R\left(\frac{\partial \ln [k_{\mathrm{H}}]}{\partial 1/T}\right)_n . \tag{3.12}$$

Therefore, the zero coverage enthalpy is simply equal to the slope of the line in Fig. 3.4b multiplied by the ideal gas constant $R = 8.314\,\mathrm{J\,mol^{-1}\,K^{-1}}$. What makes the zero coverage enthalpy so interesting is that it represents the pure sorbent-hydrogen interaction with little contribution from the hydrogen-hydrogen interactions. It can therefore be used to probe systematic trends, for example, in a series of chemically-modified carbon sorbents. However, because of the inaccuracy of low-pressure measurements the Henry's law analysis needs to be done carefully.

3.1.3 Sieverts apparatus

3.1.3.1 Description

Hydrogen adsorption measurements were collected with a custom-built, manually-operated Sieverts instrument [75]. Because the instrument is custom-built and information about it is not readily available, a detailed description will be provided in this section. The operating limits for the instrument are 100 bar and 600 ℃. A schematic drawing of the Sieverts apparatus is shown in Fig. 3.5. The instrument is equipped with both a high-resolution manometer (MKS-120, Baratron capacitance gauge, 25 000 Torr max) and a wide-range manometer (MKS-833, Baratron capacitance gauge, 3000 psi max). Temperature is monitored with platinum resistance thermometers (PRT) bonded to the exterior of the steel

[5] The deviations from linearity at small n may be due to errors in the response of the pressure transducer at very low pressures, which is then amplified by taking the algorithm. They are also sometimes characteristic of adsorption by microporous materials [6].

tubing. The vacuum system consists of a high-vacuum molecular drag pump (Alcatal MDP 5011) connected to an oil-free diaphragm backing pump (KNF, Model N880.3 AN22 E). Vacuum pressure is monitored with a cold cathode vacuum gauge. Base pressure is typically around 7×10^{-7} Torr. The instrument contains manual (DL-type) and air-actuated (HB-type) stainless steel Swagelok valves. All tubing and fittings are made from electropolished 316L stainless steel. Leak-tight Swagelok VCR® fittings are used for connections between tubing and valves. The only exception is the reactor fitting, which uses a Conflat flange copper gasket (1.33 in. flange). To prevent fine powders from being sucked into the

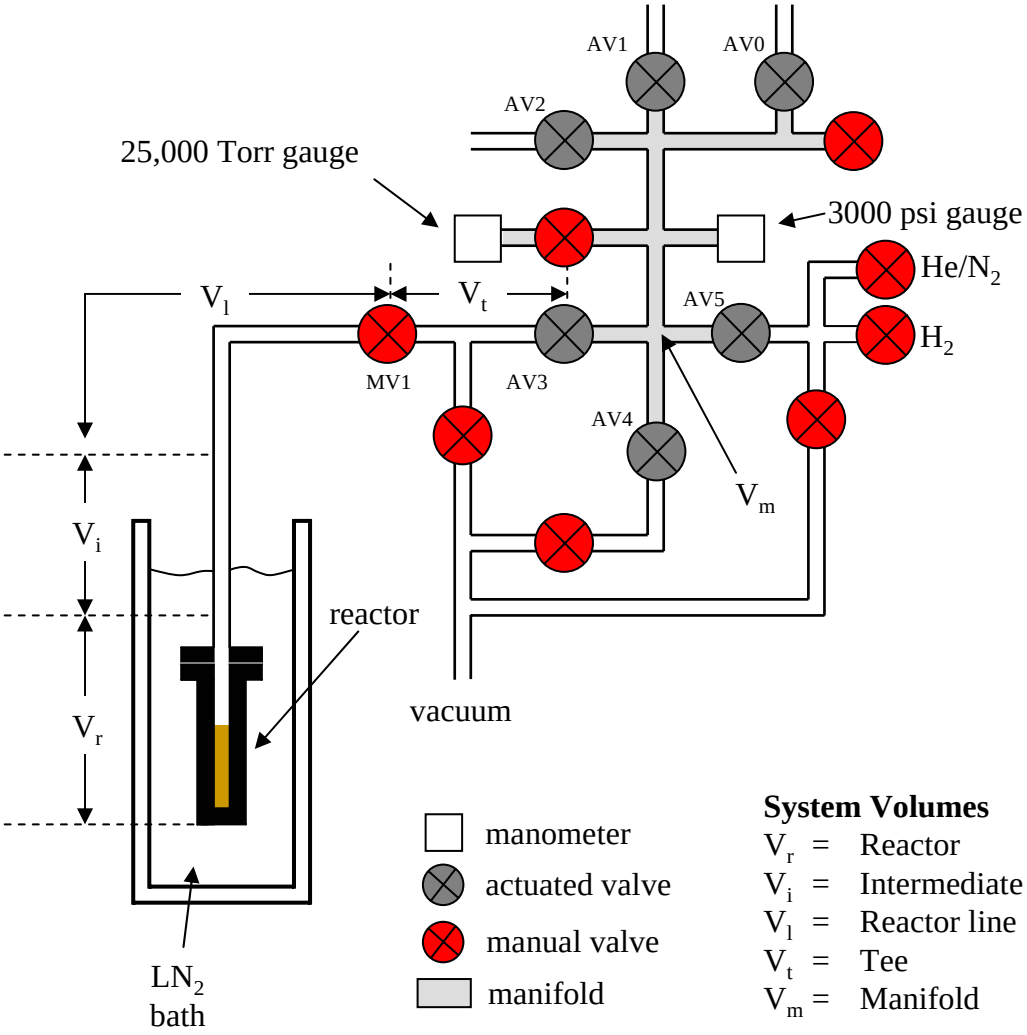

Figure 3.5: Schematic illustration of the Sieverts instrument.

manifold, a 2 µm filter gasket is typically placed into a small seat in the reactor and secured by an internal retaining ring. All components all welded, except for valves and sensors. The accuracy of the high-resolution MKS120 manometer is approximately 0.08 % of the readout, and is used with the factory calibration. The pressure gauges exhibit hysteresis, particularly following high-pressure measurements. Therefore the zero point pressure is typically reset prior to each experiment. Research-grade H_2 (99.98 %) was used for all measurements, in conjunction with an in-stream filter assembly (Millipore Corp., Inert II Reactive Micro Matrix). For air-sensitive samples, the entire reactor assembly can be brought into a glovebox and then sealed off with valve MV1 after sample loading.

3.1.3.2 Volumetric method

Measurements are collected using an extremely simple volumetric method. As pictured in Fig. 3.5, the reactor volume is kept at a constant temperature by either a liquid N_2 bath (77 K), a liquid Ar bath (87 K) or a dry ice bath (195 K). An intermediate temperature region (V_i) is assumed to have a constant temperature gradient between the bath temperature and room temperature, and is assigned an average value of $T_\mathrm{int} = (T_\mathrm{bath} + T_\mathrm{room})/2$. The remainder of the instrument volume remains at ambient room temperature, which is measured by a PRT bonded to the exterior of the manifold region. Hydrogen is first introduced into the manifold volume V_m by opening and then closing valve AV5. The gas is then expanded into the tee volume, V_t, by opening valve AV3. The pressure can be fine-tuned by opening valve AV4 and adjusting a manual needle valve which connects to the vacuum system. The initial pressure and manifold temperature are now recorded (p_1, T_room). Hydrogen is finally expanded into the reactor volume $V_\mathrm{l}+V_\mathrm{i}+V_\mathrm{r}$ by opening manual valve MV1. After allowing the adsorption system to reach equilibration (typically 15 min),

the final pressure and manifold temperature are recorded (p_2, T_{room}). Assuming it does not fluctuate too much in the course of the experiment, it is typically acceptable to use an average value of the room temperature.

Gas densities, $\rho\left(p,T\right)$, are determined from the measured pressure and temperature using the NIST Reference Fluid Thermodynamics and Transport Properties (REFPROP) database [76]. The initial and final amounts of non-adsorbed, bulk hydrogen are given by

$$n_i = \rho\left(p_1, T_{\mathrm{room}}\right)\left[V_{\mathrm{m}} + V_{\mathrm{t}}\right] \tag{3.13a}$$

$$n_f = \rho\left(p_2, T_{\mathrm{room}}\right)\left[V_{\mathrm{m}} + V_{\mathrm{t}} + V_{\mathrm{l}}\right] + \rho\left(p_2, T_{\mathrm{int}}\right)\left[V_{\mathrm{i}}\right] + \rho\left(p_2, T_{\mathrm{bath}}\right)\left[V_{\mathrm{r}} - V_{\mathrm{sample}}\right], \tag{3.13b}$$

where V_{sample} refers to the void volume displaced by the sample.[6] The surface excess adsorption is simply given by the decrease in the mass of bulk hydrogen, $n^{\sigma} = n_i - n_f$. This procedure measures the excess adsorption that occurs with a single dose of hydrogen. To collect a complete isotherm, this step is performed repeatedly at incrementally higher pressures. In the incremental method the hydrogen is not desorbed between isotherm points. This results in considerable time savings, but can also lead to incrementally increasing errors if the measurements are not done carefully. At the end of an adsorption series, we can begin a desorption series by essentially running the same procedure in reverse. With MV1 closed, the manifold + tee volume is opened to vacuum until a specific pressure is reached. Then MV1 is opened, the system is allowed to equilibrate, and the final pressure is recorded.

[6] To determine V_{sample} it is necessary to perform a set of helium expansion measurements prior to the experiment.

3.1.3.3 Errors in volumetric adsorption measurements

The volumetric method is a standard method for measuring gas adsorption and is very simple to implement. However, if adsorption measurements are collected in a cumulative fashion without desorbing between each point, errors in the data can accumulate linearly. Therefore it is important to identify all the major sources of error in a volumetric adsorption measurement.

For example, uncertainty in the void volume of the sample can to lead to large errors in the measured hydrogen adsorption, particularly for low-density materials [77]. The standard method we use to determine the void volume of the sample is to expand helium into the reactor (loaded with sample) at room temperature. It is assumed that the helium is not adsorbed and that the micropores impenetrable to helium are also impenetrable to hydrogen. I tested the accuracy of the helium volume technique on our Sieverts instrument by measuring a non-porous aluminum spacer of known dimensions. Helium was expanded into the reactor from nine different initial pressures between 1000 Torr and 9000 Torr, and measurements were simultaneously recorded using both the 25 000 Torr gauge and the 3000 psi gauge. There was considerably more variation in the measurements made by the lower resolution 3000 psi gauge. Based on its physical dimensions, the volume of the aluminum spacer was 0.99 ml. This compares to 1.01(2) ml obtained with the high-resolution gauge and 0.9(2) ml obtained with the lower resolution gauge. For many carbon adsorbents we find that it is sufficient to use a generic *skeletal density* of $2.1\,\mathrm{g\,ml^{-1}}$ (roughly the mass divided by the void volume) to calculate the void volume based on the sample mass. In cases where H_2 uptake amounts are large, we can use this approximation.

If single-point measurements are collected for long time periods (i.e., several hours), then daily fluctuations in the ambient temperature can affect the data in several ways. First,

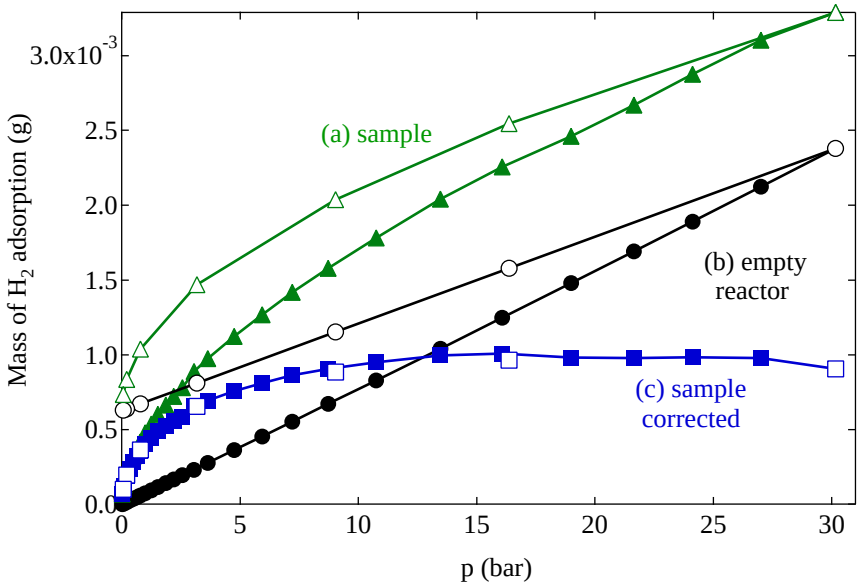

Figure 3.6: Illustration of the effect of empty reactor adsorption. (a) Hydrogen adsorption by reactor containing a sample (Cr_2O_3 aerogel). (b) Adsorption by the empty reactor. (c) Corrected sample adsorption after subtracting the empty reactor background. Sample temperature was 77 K and pressure was measured on the high-resolution gauge. Solid symbols are adsorption points and open symbols are desorption points. Total H_2 adsorption amount is presented rather than the specific adsorption amount.

the hydrogen density in the manifold can change slightly, which can be significant at high pressures. Second, the signals from the capacitance pressure gauges themselves change with temperature. Leaks within the system can also cause problem for measurements that involve either long collection times or small adsorption amounts. To test these temperature effects, I filled the instrument volume with H_2 and logged all system temperatures and pressures for up to 80 hours. At 50 bar pressure there were not any detectable leaks in the system, and the pressure was well-correlated with the ambient temperature. There did appear to be a leak at 80 bar, in which the pressure dropped substantially without any correlation with the ambient temperature. Therefore leaks can indeed be a major source of error on this instrument at high pressures. Fortunately none of the adsorption measurements presented in this thesis exceed 50 bar pressure.

A useful way to determine the accuracy of the Sieverts instrument is to collect a hydrogen

adsorption isotherm with an empty reactor. If the reactor is at 298 K, there should be no real adsorption. Any measured adsorption is due to experimental errors. If the reactor is at 77 K or 87 K, there may be a small amount of adsorption on the reactor walls or in the filter gasket mesh, but any substantial measured adsorption is indicative of cumulative error. We have performed numerous empty reactor measurements at the standard sample temperatures. An illustrative example of the effect of empty reactor adsorption is presented in Fig. 3.6. In this case the total H_2 adsorption by the sample (a Cr_2O_3 aerogel) was very small, on the order of the empty reactor adsorption itself. To determine the true adsorption by the sample, the background adsorption by the empty reactor needs to be subtracted. Hysteresis is present for the empty reactor adsorption and desorption runs, so they need to be fit to separate linear equations. The corrected sample adsorption and desorption is obtained once the reactor background has been subtracted.

3.2 Neutron scattering

3.2.1 Introduction

Neutron scattering is a powerful method for investigating the structure and dynamics of condensed matter. It is particularly useful as a tool for studying H_2 as a guest species inside of a host adsorbent. There are several reasons for this. First, compared to electrons and X-rays, neutrons interact weakly with matter. This means that they can probe the hydrogen dynamics within bulk materials instead of simply being scattered at the surface. Second, hydrogen contains a comparatively large neutron scattering cross-section. Neutrons are scattered by nuclear forces, and the scattering cross-sections do not vary systematically with the atomic number Z. This is different than X-ray scattering cross-sections, which vary

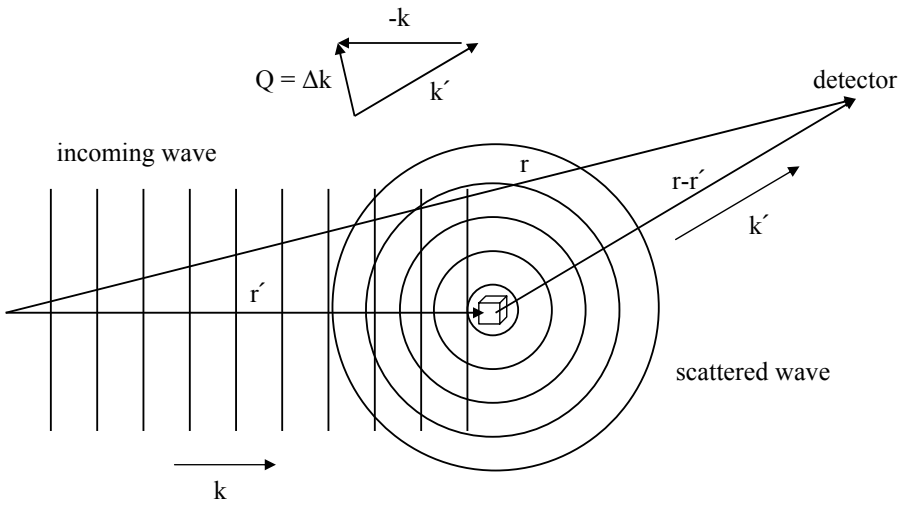

Figure 3.7: Wavevectors and position vectors for a neutron scattering event. The vector **Q** is defined as $\mathbf{k}' - \mathbf{k}$ at the top-center of the illustration. Adapted from Ref. [78].

with Z^2. Therefore, even in a carbon adsorbent system consisting of only 1% hydrogen by mass, more than half of the neutron scattering is due to hydrogen. Finally, thermal neutrons conveniently have wavelengths similar to the interatomic distances in solids and kinetic energies on the order of excitations in condensed matter (e.g., phonons). In this section, a brief overview of neutron scattering theory will be presented as well as an introduction to the instrumental methods used to collect the data.

3.2.2 Theory

A neutron scattering event with a single nucleus is illustrated in Fig. 3.7. Neutrons have both particle-like and wave-like properties. The incident neutron can be described by a plane wave $\psi_{inc} = e^{i(\mathbf{k}\cdot\mathbf{r}'-\omega t)}$. The wavefunction of the scattered neutron emanates from the center of the scattering and is described by a spherical wave $\psi_{sc} = \frac{b}{|\mathbf{r}-\mathbf{r}'|}e^{ik'|\mathbf{r}-\mathbf{r}'|}$, where b is the scattering length of the nucleus. The neutron wavevector $\mathbf{k}$ points in the direction of the velocity and has the magnitude $k = 2\pi/\lambda$, where λ is the de Broglie wavelength. The neutron momentum is $\mathbf{p} = \hbar\mathbf{k}$ and the energy is $E = \frac{1}{2m}\hbar^2k^2$. For the scattered neutron,

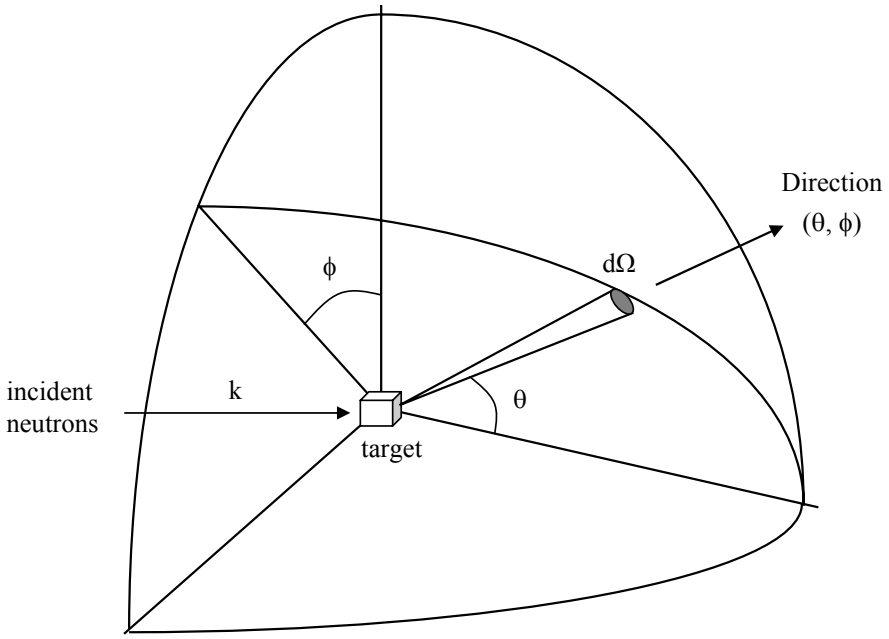

Figure 3.8: Simplified layout of the typical geometry of a neutron scattering experiment. Adapted from Ref. [79].

the momentum transfer has the magnitude

$$\hbar\mathbf{Q} = \hbar\left(\mathbf{k}' - \mathbf{k}\right), \tag{3.14}$$

and the neutron energy transfer is

$$\hbar\omega = E' - E = \frac{\hbar}{2m}\left(k'^2 - k^2\right). \tag{3.15}$$

The momentum transfer depends both on the scattering angle and the energy transfer. The wavevector transfer $\mathbf{Q}$ is often used to represent the momentum transfer (especially in figure annotations) and is reported in units of Å^{-1}. When the sample is at low temperatures, the scattered neutrons typically lose energy, but $\hbar\omega$ is typically still reported as a positive quantity to denote energy loss (the convention used in this thesis).

The quantity that is directly measured in a neutron scattering experiment is the double

differential cross-section. As illustrated in Fig. 3.8, the neutrons are incident on some target. They have a known initial energy E and a known flux Φ. What the neutron spectrometer typically measures is the number of neutrons of final energy E' scattered in a particular direction (θ, ϕ). This quantity can be formalized by considering the double differential cross-section, $\mathrm{d}^2\sigma/\mathrm{d}\Omega\mathrm{d}E$, which gives the number of neutrons scattered per second into the solid angle $\mathrm{d}\Omega$ with a final energy in the range $\mathrm{d}E$, divided by the incident flux Φ. The cross-section has dimensions of [area] and is typically expressed in units of barn, where $1\,\mathrm{b} = 10^{-28}\,\mathrm{m}^2$. The total scattering by the nucleus is obtained by integrating over solid angle and energy,

$$\sigma = \int \mathrm{d}E \int \mathrm{d}\Omega \frac{\mathrm{d}^2\sigma}{\mathrm{d}\Omega\mathrm{d}E} = 4\pi b^2, \tag{3.16}$$

where b is the scattering length of the nucleus.

We do not study scattering from a single nucleus but from a large system of scatterers. Even if the system consists of a single element, the scattering length b_i of each individual nuclei can differ depending on nuclear spin or the presence of isotopes. This leads to the presence of coherent and incoherent scattering from a sample. The coherent and incoherent cross-sections are given by

$$\sigma_{\mathrm{coh}} = 4\pi\langle b\rangle^2 \tag{3.17}$$

$$\sigma_{\mathrm{inc}} = 4\pi\left(\langle b^2\rangle - \langle b\rangle^2\right). \tag{3.18}$$

Incoherent scattering arises from random deviations of scattering lengths from their mean value. The hydrogen isotope ^{1}H has oppositely signed scattering lengths for its two nuclear spin states ($\pm\frac{1}{2}$) with a weighted mean close to zero. It is therefore an overwhelmingly incoherent scatterer. In incoherent scattering, the phase relationship between the incident

wave and the scattered wave is not preserved. We cannot directly sum the scattered waves to obtain the total outgoing wave. Instead, we sum the individual intensities of the scattered waves to obtain the total incoherent intensity,

$$I_{\text{inc}} = \sum_{\mathbf{r}_i} I_{\mathbf{r}_i} = \sum_{\mathbf{r}_i} |\psi_{\mathbf{r}_i}|^2. \tag{3.19}$$

The waves do not interfere constructively or destructively and do not provide direct information on the material structure. However, incoherent scattering does provide information on the self-correlation function of the scatterers. The van Hove self-correlation function, $G_{\text{s}}(\mathbf{r}, t)$, can be interpreted as giving the probability that a particle will be found at position $\mathbf{r}(t)$ at time t if it was initially located at the origin at time zero. The incoherent scattering function, $S_{\text{inc}}(\mathbf{Q}, \omega)$, is the Fourier transform in time and space of the van Hove self-correlation function:

$$S_{\text{inc}}(\mathbf{Q}, \omega) = \frac{1}{2\pi} \iint \exp\left[i\left(\mathbf{Q} \cdot \mathbf{r} - \omega t\right)\right] G_{\text{s}}(\mathbf{r}, t)\, \mathrm{d}\mathbf{r}\mathrm{d}t. \tag{3.20}$$

The quantity which is actually measured by the instrument, however, is the double differential scattering cross-section,

$$\left(\frac{\mathrm{d}^2\sigma}{\mathrm{d}\Omega \mathrm{d}E'}\right)_{\text{inc}} = \frac{\sigma_{\text{inc}}}{4\pi\hbar}\frac{k'}{k} S_{inc}(\mathbf{Q}, \omega) \tag{3.21}$$

from which $S_{\text{inc}}(\mathbf{Q}, \omega)$ is typically extracted (to within some arbitrary prefactor). In this context, $\mathbf{Q}$ and ω are the spatial and temporal frequencies obtained by Fourier transform from the real-space variables $\mathbf{r}$ and t. Measurements at small $\mathbf{Q}$ are therefore sensitive to processes with large characteristic lengths. Similarly, measurements at small energy loss $\hbar\omega$

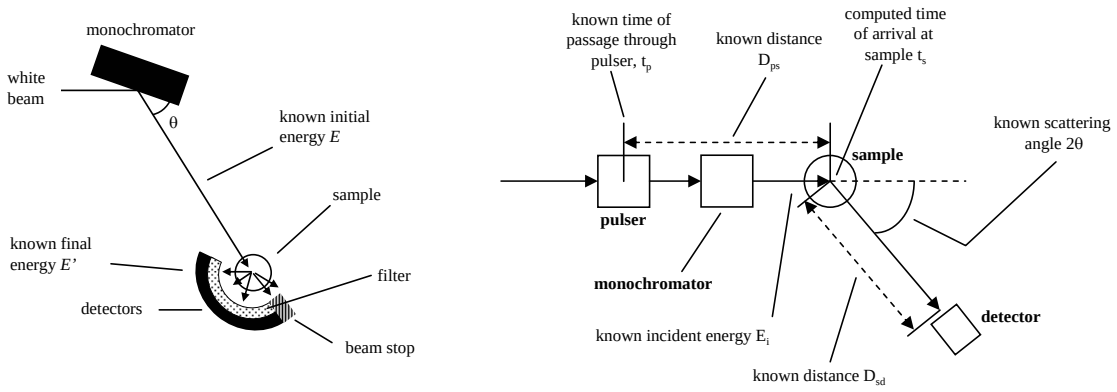

(a) Inverse Geometry **(b) Direct Geometry**

Figure 3.9: Schematic illustration of (a) an inverse geometry neutron spectrometer and (b) a direct geometry spectrometer.

correspond to slow processes with large characteristic times, τ.

3.2.3 Indirect geometry spectrometers

An instrument with a fixed final neutron energy is called an inverse geometry spectrometer. The Filter Analyzer Spectrometer (FANS) instrument at the NIST Center for Neutron Research (NCNR) is an example of an inverse geometry instrument [80]. This instrument was used for most of my inelastic measurements on KC_{24}, and a schematic is illustrated in Fig. 3.9a. An incoming white beam contains a distribution of wavelengths. The crystal monochromator selects a particular wavelength at the angle θ by Bragg diffraction. The initial neutron energy is then given by $E = h^2/\left(2m\lambda^2\right)$. The sample is moved step-wise across a range of θ which allows the initial energy to be varied. The final energy is fixed by a low-pass graphite/beryllium filter which has a cutoff of around $E' = 1\,\text{meV}$. Data is collected at each angle, θ, for a specific number of monitor counts, and the neutrons which reach the detector during this interval are known have an energy loss of about E, with the resolution set primarily by the low-pass filter. At each step counts are summed over the entire pie-shaped detector array. Due to the low final energy, however, the final wavevector

is negligible compared to the initial wavevector and therefore $\mathbf{Q}$ is largely independent of the scattering angle (i.e., $\mathbf{Q} \approx \mathbf{k}$). This means that $E \sim Q^2$ and that peaks at large energy also have a large Q. What is measured is not actually the scattering function, $S_{\text{inc}}(\mathbf{Q}, \omega)$, but a quantity which is approximately proportional to the vibrational density of states of the sample.

3.2.4 Direct geometry spectrometers

Direct geometry spectrometers use a chopper to produce a neutron beam with fixed initial energy. As illustrated in Fig. 3.9b, the final neutron energy is calculated from the time-of-flight from the sample to the detector. From the angle of the detector, and the initial and final energies, the magnitude of the momentum transfer can be calculated:

$$\frac{\hbar^2 Q^2}{2m} = E + E' - 2\left(EE'\right)^{1/2} \cos\theta. \tag{3.22}$$

Based on position, each detector has a different trajectory through (Q, ω) space. It is important to normalize the detector efficiencies by measuring the scattering from a purely incoherent scatterer such as vanadium. The Disc-Chopper Spectrometer (DCS) at NCNR is an example of a direct-geometry spectrometer [81]. It was used for most of the quasielastic measurements on KC_{24}. Because it is located at a reactor neutron source, it has a disc chopper component to artificially create a pulsed source.